Chapter 5

Bis(*m*-phenylene)-32-Crown-10-Based Cryptands, Powerful Hosts for Paraquat Derivatives

5.1. INTRODUCUTION

Self-assembled structures are attractive to materials science for their reversibility at the molecular level, and therefore for their ability to correct structural defects, an option unavailable for traditional, covalently bonded systems.[1] However, in order for a self-assembling, non-covalent system to possess properties sufficient to compete with covalently bonded polymers, it must exhibit a strong association between its components.[2] Paraquat derivatives (*N*,*N*'-dialkyl-4,4'-biyridinium salts) have been widely used as guests in supramolecular chemistry to construct numerous complexes with large crown ethers, such as bis(*m*-phenylene)-32-crown-10 derivatives and bis(*p*-phenylene)-34-crown-10 derivatives.[3] With the aim to prepare large supramolecular systems[4] efficiently from small building blocks, we are interested in improving complexation of paraquats by design of optimized hosts. Here, by synthesizing four new cryptands and studying their complexation with paraquat derivatives, we address two questions. First, why are cryptands better hosts for paraquat derivatives than the corresponding simple crown ethers? Second, can we further improve complexation by introducing more and/or better binding sites?

5.2. RESULTS AND DISCUSSION

A. Design of Cryptands.

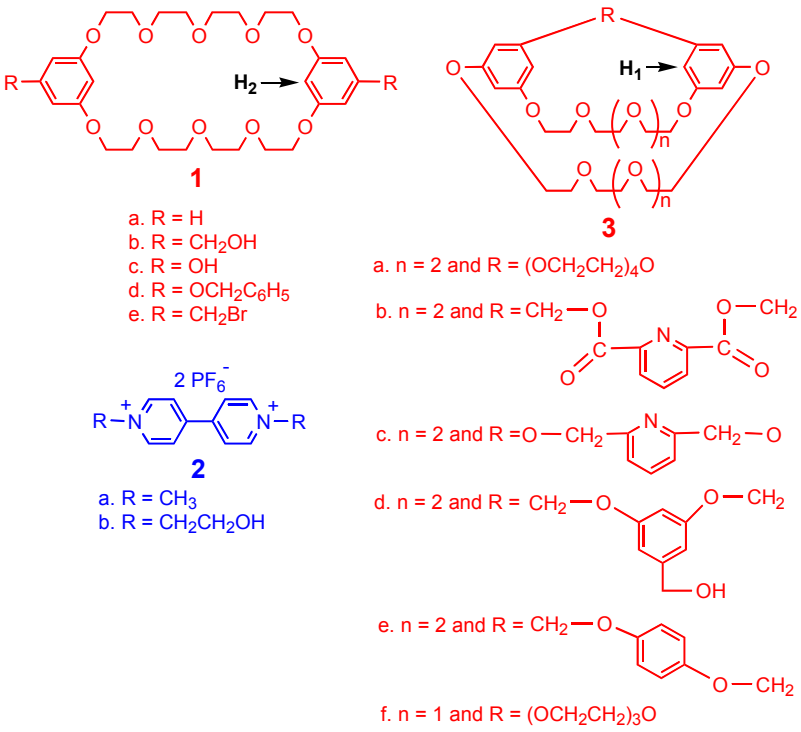

We reported that cryptand **3a** exhibited a 100-fold increase in association constant (K_a) for paraquat derivatives **2** relative to crown ether **1a**.[5a] The enhanced association in the case of **3a** is due to the preorganization[6] of the host. This was confirmed by the thermodynamic study of four complexes based on **1c**,[5a] **1d**,[5a] **2a**,[5a] **2b**,[5a] and **3a**[5a] (Table 1). Interestingly, the enthalpies of binding of crowns **1c** and **1d** are comparable to or larger than that of cryptand **3a**, but the entropic penalties for the crown ethers are much larger than for the cryptand. As expected the cryptand **3a** undergoes significantly less structural change in the analogous process and this is the major factor in its enhanced binding strength.

Table 1. Association constants[a] and thermodynamic parameters[b] for complexes of paraquat derivatives (**2a** and **2b**) with crown ethers (**1c** and **1d**) and a cryptand (**3a**).

Complex	$K_a \times 10^{-2}$ (M^{-1})	ΔG_{294K}[c] (kJ/mol)	ΔH_a[d] (kJ/mol)	ΔS_a[d] (J/mol•deg)
3a•2a	6.0×10^2	-25	-48	-78
3a•2b	6.0×10^2	-25	-54	-97
1c•2b	2.7 ± 0.5	-14	-48	-117
1d•2b	3.5 ± 0.5	-14	-56	-144

a. Measured at 21°C; average of 5 solutions with the constant host concentration and varying guest concentrations ($[guest]_0$:$[host]_0$ = 1-50). K_a values of complexes of **3a** were determined before[5a] and the same method was used for complexes of **2b** using the time averaged signals for H_2 of **1c** and **1d**.

b. Determined by variable temperature ^{1}H NMR spectroscopy in acetone-d_6 and van't Hoff plots using the time averaged signals for H_1 of **3a** and H_2 of **1c** and **1d**.

c. Estimated error: ±5% relative.

d. Measured from 21-50°C; estimated errors: < 10% relative.

This is consistent with the X-ray analysis results that bis(*m*-phenylene)-32-crown-10 (**1a**) is not folded in the solid state,[3a] but it and its derivative **1b** are folded in crystalline complexes with paraquat **2a** (Figure 1a),[5a] a paraquat derivative,[3e] and a diammonium salt.[7] Formation of pseudocryptands using ditopic counterions, such as trifluoroacetate,[8] water,[9a] or trifluoroacetate and water together,[9b] to hydrogen bond the OH groups of **1b**[8,9a] or **1c,**[9b] is also effective in increasing association constants for such "taco complexes".

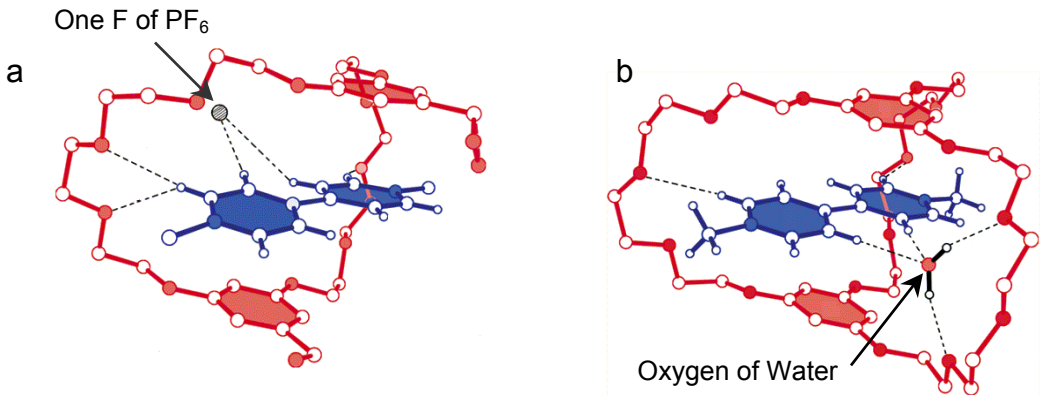

Figure 1. X-ray structures of **1b•2a** (a) and **3a•2a** (b).[5a]

Our continuing design of improved paraquat hosts is based on careful examination of the X-ray structures. Note from the structure of the cryptand complex **3a•2a** (Figure 1b) the lack of direct interaction of the guest with the third ethyleneoxy chain of **3a**. Rather the β-pyridinium hydrogens of **2a** are bound to a water molecule that bridges to the ether oxygen atoms of the third ethyleneoxy chain. Moreover, in crown ether based **1b•2a** (Figure 1a) an F atom of the PF_6 counterion is H-bonded to the β-pyridinium hydrogens of **2a**. On the basis of these observations we designed new cryptands **3b** and **3c** with an H-bond acceptor site, the pyridyl nitrogen, in approximately the proper location for interaction with the β-pyridinium hydrogens of **2a**. In **3b** the third linker between the phenylene rings contains nine atoms, while in **3c** it contains only seven atoms. The pyridine ring of **3b** is affected by the electron withdrawing carbonyl groups, while that of **3c** is more electron-rich because of the CH_2O substituents. Cryptand **3d** has the same length of the third bridge as cryptand **3c**, but **3d** has no additional binding site on the third bridge. Comparison of the complexation of these two cryptands with paraquat will reveal the importance of the additional binding site. Cryptand **3e** was prepared with the aim to optimize the length of the third bridge; the number of atoms in the third bridge of cryptands **3b**, **3c**, **3d**, and **3e** is 9, 7, 7, and 8, respectively. Thus, these structures address two issues: geometry and intrinsic H-bonding ability of the host.

B. Syntheses of Cryptands, 3b, 3c, 3d, and 3e.

All four new cryptands, **3b**, **3c**, **3d**, and **3e**, were prepared using the pseudo-high dilution technique. Bis(1,3,5-phenylene)di(1',4',7',10',13'-pentaoxatridecyl)[2'',6''-di(methyleneoxycarbonyl)pyridine] (**3b**) was synthesized from bis(5-hydroxymethyl-1,3-phenylene)-32-crown-10[10] (**1b**) and 2,6-pyridinedicarbonyl dichloride. Bis-(1,3,5-phenylene)di(1',4',7',10',13'-pentaoxatridecyl)(2'',6''-dioxymethylenepyridine) (**3c**) was made from bis(5-hydroxy-1,3-phenylene)-32-crown-10[5a] (**1c**) and 2,6-bis(bromomethyl)pyridine. Bis(1,3,5-phenylene)di(1',4',7',10',13'-pentaoxatridecyl)[3'',5''-di(methyleneoxy)benzyl alcohol] (**3d**) was prepared from bis(5-bromomethyl-1,3-phenylene)-32-crown-10[10] (**1e**) and 3,5-dihydroxybenzyl alcohol. Bis(1,3,5-phenylene)di(1',4',7',10',13'-pentaoxatridecyl)[1'',4''-di(methyleneoxy)benzene] (**3e**) was prepared from **1e** and hydroquinone.

C. Complexation of the New Cryptands with paraquat (2a).

For each of the four new cryptands **3b**, **3c**, **3d**, and **3e**, a 1.00 mM equimolar acetone solution of the cryptand and **2a** is yellow due to charge transfer between electron-rich aromatic rings of the cryptand host and electron-poor pyridinium rings of the guest **2a**. Job plots[11] (Figure 2) based on proton NMR data demonstrated that all four complexes were of 1:1 stoichiometry in solution.

a

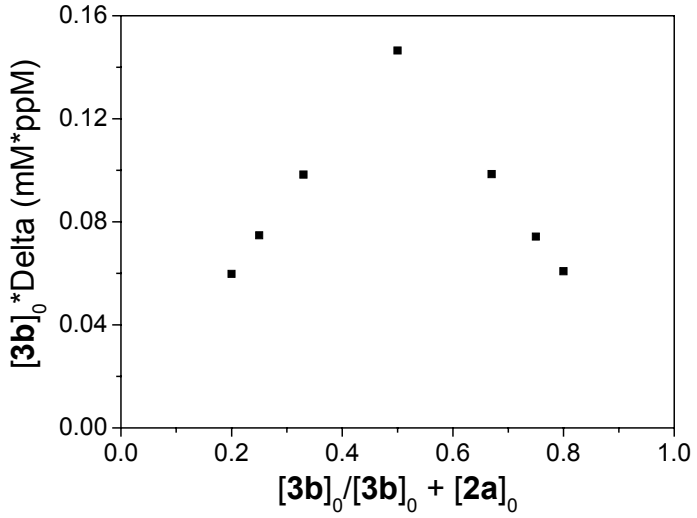
0.16
0.12
0.08
0.04
0.00
0.0
0.2
0.4
0.6
0.8
1.0
[3b]0*Delta (mM*ppM)
[3b]0/[3b]0 + [2a]0

b

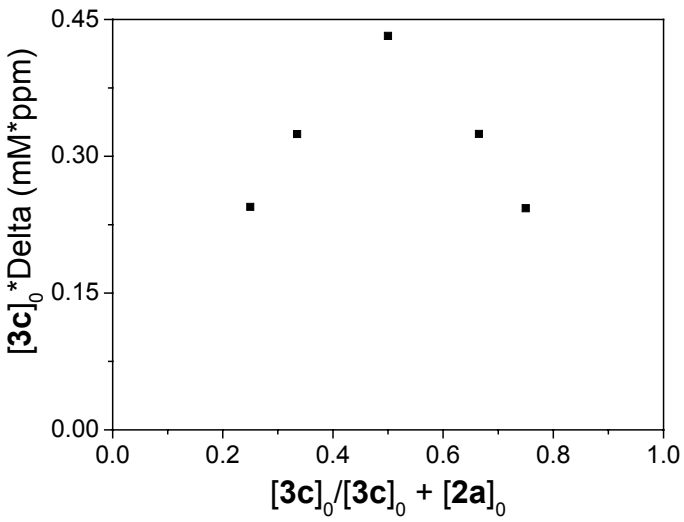
0.45
0.30
0.15
0.00
0.0
0.2
0.4
0.6
0.8
1.0
[3c]0*Delta (mM*ppm)
[3c]0/[3c]0 + [2a]0

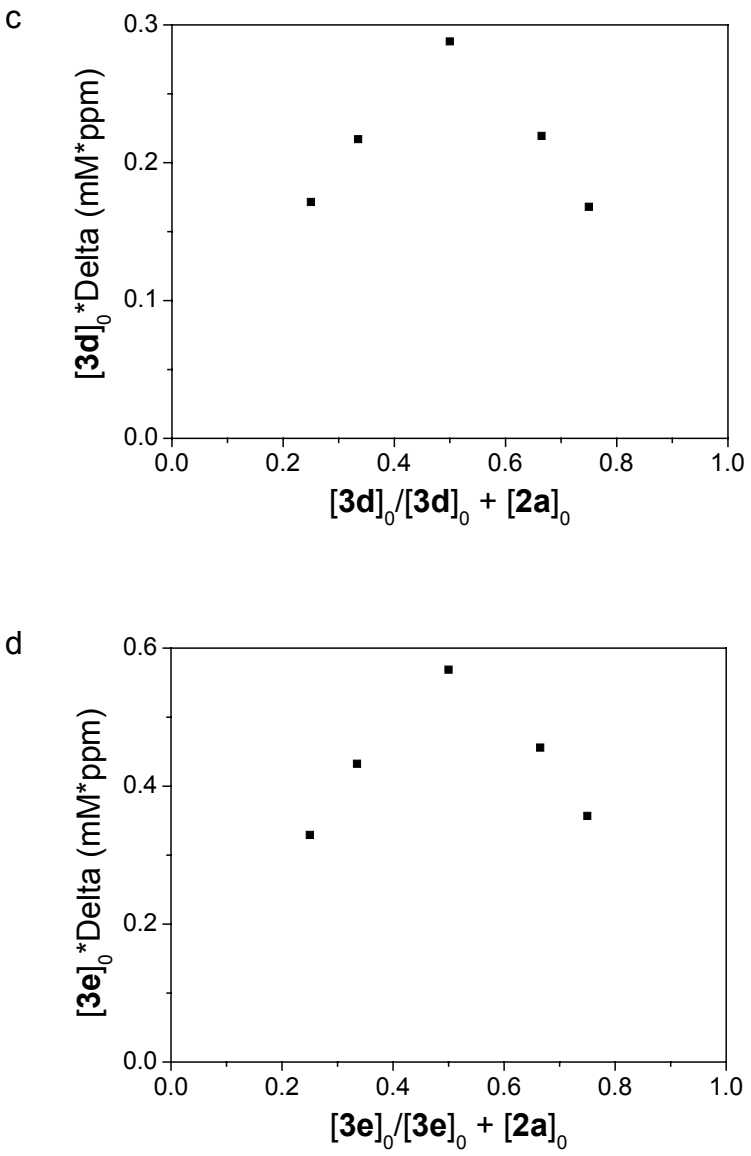

Figure 2. Job plots showing the 1:1 stoichiometries of the complexes between **3b** and **2a** (a), between **3c** and **2a** (b), between **3d** and **2a** (c), and between **3e** and **2a** (d) in CD_3COCD_3. (a) $[\mathbf{3b}]_0 + [\mathbf{2a}]_0 = 1.00$ mM; (b) $[\mathbf{3c}]_0 + [\mathbf{2a}]_0 = 2.00$ mM; (c) $[\mathbf{3d}]_0 + [\mathbf{2a}]_0 = 2.00$ mM; (d) $[\mathbf{3e}]_0 + [\mathbf{2a}]_0 = 2.00$ mM**.** $[\mathbf{2a}]_0$, $[\mathbf{3b}]_0$, $[\mathbf{3c}]_0$, $[\mathbf{3d}]_0$, and $[\mathbf{3e}]_0$ are initial concentrations of **2a**, **3b**, **3c**, **3d**, and **3e**. Delta = chemical shift change for H_1 of **3b**, **3c,** **3d**, and **3e**.

The association constant K_a for the complexation between **3b** and **2a**, a fast-exchange system, was determined to be 5.0 (± 2.0) × 10^6 M^{-1} in acetone-d_6 at 22 °C. using a competitive complexation method recently developed by Smith group.[12] This value is one of the highest for association constants of paraquat complexes.[5,13] K_a values for the other complexes are summarized in Table 2. Compared with the K_a value of **1a•2a**, the complex based on the simple crown ether, K_a values of cryptand complexes **3b•2a**, **3c•2a**, **3d•2a**, and **3e•2a** increased about 9000, 17, 11, and 40 times, respectively.

Table 2. Association constants in acetone-d_6 for complexes of paraquat **2a** with crown ether **1a** and different cryptands at 22 °C.

	1a•2a[a]	**3b•2a**	**3c•2a**	**3d•2a**	**3e•2a**
$K_a \times 10^{-3}$ (M^{-1})	0.55 (±0.05)	5.0 (±2.0) × 10^3	9.4 (±0.9)	6.3 (±0.6)	22 (±2)

a. K_a of complex **1a•2a** was reported before.[14]

The improvement from crown ether complex **1a•2a** to cryptand complexes **3d•2a** and **3e•2a** can be mainly attributed to the preorganization of the cryptand hosts, while the improvement from **3d•2a** to **3c•2a** is due to the introduction of an additional binding site, the pyridyl nitrogen atom. The great increase in association constant from crown ether complex **1a•2a** to pyridyl ester cryptand complex **3b•2a** is a result of the combination of the preorganization of the host and the introduction of an additional binding site. The increase in association constant from pyridyl ether cryptand (7-atom link) complex **3c•2a** to hydroquinone cryptand (8-atom link) complex **3e•2a** and to pyridyl ester cryptand (9-atom link) complex **3b•2a** indicates that nine is an appropriate number of atoms on the third bridge of the cryptand host for the best complexation of paraquat derivatives.

D. Solid State Structures of 3b and [2]Complex 3b•2a.

The X-ray crystal structures of pyridyl ester cryptand **3b** and paraquat **2a** are shown in Figures 3a and 3b and that of their complex **3b•2a** is shown in Figure 3c. No solvent molecules were found in the structure of **3b**. The two phenylene rings of **3b** are

not parallel to each other but exhibit a twist angle of 36°. The centroid-centroid distance between them is 6.68 Å. Most notably, in accord with our design, a β-pyridinium hydrogen of the guest is directly H-bonded to the pyridine nitrogen atom of the host in **3b•2a** (**E**)**.** That is, the pyridine nitrogen atom of **3b** in **3b•2a** is at almost the same position as the oxygen atom of the water bridge in **3a•2a** and the fluorine atom of a PF_6^- anion in **1b•2a** (Figure 1). On the other side of **2a**, both β-pyridinium hydrogens are hydrogen-bonded to the oxygen atom of an acetone molecule (**A** and **B**). Just like **3a•2a** (Figure 1b),[5a] **3b•2a** is stabilized by two hydrogen bonds involving α-pyridinium hydrogens (**C** and **J**). However, N-methyl hydrogens are not involved in hydrogen bonding in **3a•2a**, but there is one hydrogen bond involving a methyl hydrogen in **3b•2a** (**I**). One possible reason for this difference is that the third bridge (9 atoms) of **3b** is shorter than that (13 atoms) of **3a** and this allows the guest to be closer to the ethyleneoxy links. Further stabilization forces are four indirect hydrogen bonds (**D**, **F**, **G**, and **H** in Figure 3c) between **3b** and **2a** based on two acetone bridges. The two oxygen atoms on the acetone bridges are hydrogen bonded to different phenyl hydrogens of the cryptand (**D** and **H**) and the same α-pyridinium hydrogen (**F** and **G**). Comparison of the crystal structures of **3b** and **3b•2a** (Figures 3b and 3c) shows that the conformation of the host does not change much during complexation because of its preorganization.[6] Therefore, the enhanced affinity of **3b** for **2a** is attributable to its preorganization and the properly located additional binding site.

It is not surprising that, just like **3a•2a**,[5a] **3b•2a** is also stabilized by face-to-face π-stacking interactions. For maximizing π-stacking interactions between the cryptand host **3b** and the paraquat guest **2a**, the aromatic rings of **3b** are almost parallel, with an angle of 7.4° and a centroid-centroid separation of 7.19 Å while the corresponding values are 9.8° and 6.94 Å in **3a•2a**;[5a] the paraquat guest **2a** lies nearly parallel to and nearly symmetrically between the two phenylene rings of **3b**.

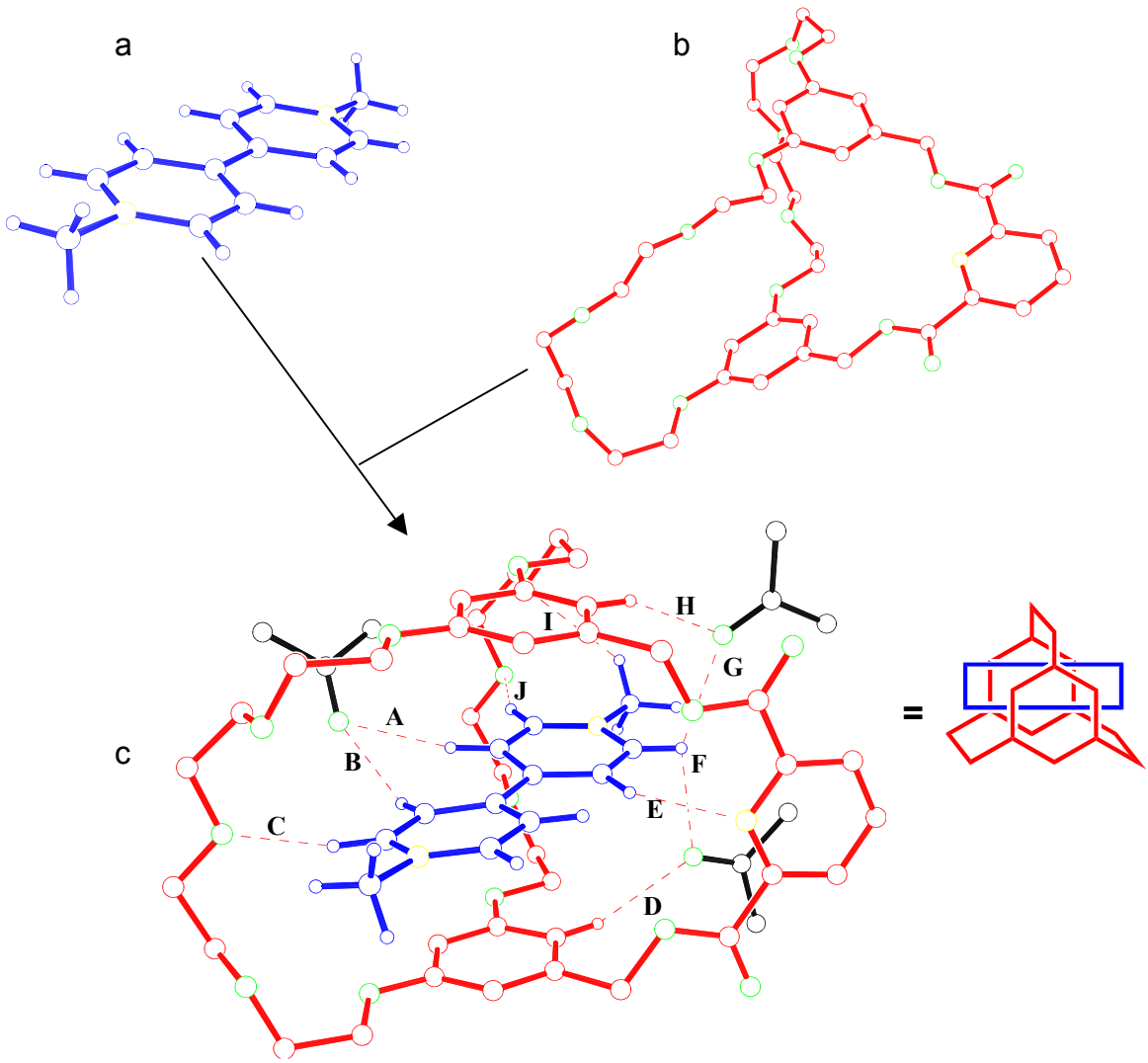

Figure 3. X-ray structures of **2a** (a), **3b** (b), and **3b•2a** (c). Oxygens are green, nitrogens are yellow, acetone molecules are black, **3b** is red, and **2a** is blue. (a) Two PF_6^- ions have been omitted for clarity. (b) and (c) Hydrogens of **3b**, the other solvent molecules, and PF_6^- ions have also been omitted for clarity. Hydrogen-bond parameters: C···O(N) distances (Å), H···O(N) distances (Å), C-H···O(N) angles (deg) **A**, 3.33, 2.35, 166; **B**, 3.22, 2.38, 141; **C**, 3.05, 2.08, 163; **D**, 3.53, 2.57, 162; **E**, 3.22, 2.37, 142, **F**, 2.84, 2.53, 97.0; **G**, 2.99, 2.50, 110; **H**, 3.52, 2.57, 157; **I**, 3.42, 2.61, 138; **J**, 3.41, 2.48, 155. Face-to-face π-stacking parameters: centroid-centroid distances (Å) 3.82, 4.15, 4.25, 4.53; ring plane/ring plane inclinations (deg): 5.4, 2.8, 12.6, 5.0.

E. Solid State Structure of [3]Complex 3c•2a•3c.

Though the complex between pyridyl ether cryptand **3c** and **2a** has 1:1 stoichiometry in solution as shown above and the gaseous state as shown below and the molar ratio of host:guest in the mother solution for the crystal growth was 1:2, the complex between **3c** and **2a** have 2:1 stoichiometry in the solid state (Figure 4). **3c•2a•3c** is similar to two recently reported pseudorotaxane-like complexes,[14] **3a•2a•3a** and **3f•2a•3f**, in that each paraquat unit is shared by two cryptand moieties and the dihedral angle between two pyridinium rings of the paraquat guest is zero. However, in **3c•2a•3c** two N-methyl hydrogens are involved in hydrogen bonding to the hosts (**Q**), while no N-methyl hydrogens in **3a•2a•3a** and **3f•2a•3f** are involved in hydrogen bonding. Also in **3c•2a•3c** there are two acetonitrile molecules, while in **3a•2a•3a** there are two water molecules and in **3f•2a•3f** from the smaller cryptand **3f** there are no solvent molecules. Notably again, the pyridyl nitrogen atom is hydrogen bonded to the β-pyridinium hydrogen atoms in **3c•2a•3c** (**M** and **N**). It appears that the 2:1 complex maximizes H-bonding in the solid state; it produces 4 α-pyridinium to host (**O** and **P**), 4 bifurcated β-pyridinium to host (**M** and **N**), 2 methyl to host (**Q**), 2 methyl to acetonitrile (**K**), and 2 α-pyridinium to acetonitrile H-bonds (**L**). In solution presumably some of these pyridinium hydrogens can interact with solvent molecules so the complex between **3c** and **2a** has the 1:1 stoichiometry.

CPK model studies suggest that when 1:1 complexes are formed, the pyridine nitrogen of cryptand **3b** is at a better position to form hydrogen bonds with the β-pyridinium hydrogens of the paraquat derivatives than that of **3c**, because of the difference in the third bridge lengths-9 atoms for **3b** and 7 atoms for **3c**. Furthermore, when forming 1:1 complexes with paraquat derivatives, the two phenylene rings of the smallest host **3c** can not be parallel to each other because of the shorter third bridge, while those of **3b** can do so. This makes face-to-face π-stacking interactions weaker in **3c•2a** than in **3b•2a**. These factors lead to an 840-fold increase in the value of apparent association constant from **3c•2a** to **3b•2a** even though the pyridine ring of **3c** is presumably a better donor than that of **3b**.

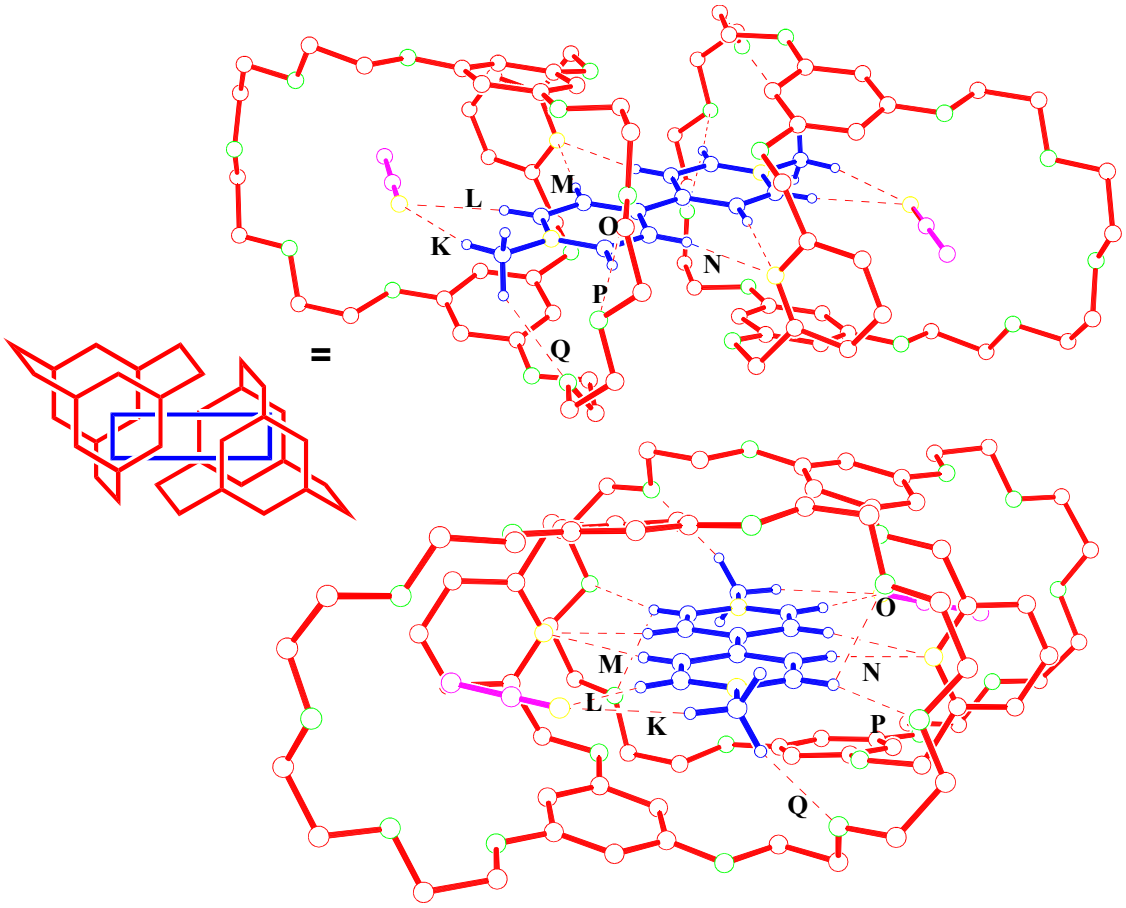

Figure 4. Two views of the X-ray structure of **3c•2a•3c**. Oxygens are green, nitrogens are yellow, **3c** is red, **2a** is blue, and acetonitrile molecules are magenta. The other solvent molecules, two PF_6^- ions, and hydrogens except the ones on **2a** have been omitted for clarity. Hydrogen-bond parameters: C···O(N) distances (Å), H···O(N) distances (Å), C-H···O(N) angles (deg) **K**, 3.49, 2.56, 161; **L**, 3.41, 2.53, 157; **M**, 3.55, 2.61, 175; **N**, 3.31, 2.38, 168; **O**, 3.07, 2.51, 118; **P**, 3.35, 2.45, 162; **Q**, 3.32, 2.50, 143. Face-to-face π-stacking parameters: centroid-centroid distances (Å) 3.85, 4.16; ring plane/ring plane inclinations (deg): 8.9, 15.5. The centroid-centroid distance (Å) and dihedral angle (deg) between the pyridinium rings of **2a**: 4.27 and 0.

F. Solid State Structure of [2]Complex 3d•2a.

As shown by its crystal structure (Figure 5), **3d•2a** is stabilized by H-bonding and face-to-face π-stacking interactions. However this complex has some unique characterics which were not observed in previously reported 1:1 cryptand/paraquat complexes[5a,15] and **3b•2a**. Firstly, the paraquat guest **2a** is threaded unsymmetrically into the cavity of the 32-crown-10 part of the cryptand host in **3d•2a** (Figure 5), while the paraquat unit is nearly symmetrically located in all other reported 1:1 cryptand/paraquat complexes[5a,15] and **3b•2a**. The unsymmetrical orientation in **3d•2a** results from H-bonding of one of the α-hydrogens of **2a** with the benzyl ether oxygen of **3d** (**S** of Figure 5) and intercomplex H-bonding (see below and Figure 6). Secondly, due to the unsymmetrical threading, the phenylene rings of the 32-crown-10 part are face-to-face π-stacked with only one pyridinium ring of the guest (Figures 5 and 6), while in all other reported 1:1 cryptand/paraquat complexes[5a,15] and **3b•2a** the phenylene rings are face-to-face π-stacked with both pyridinium rings of the guest. Thirdly, the dihedral angle, 21.4°, between the pyridinium rings (Figure 5) is the largest among reported 1:1 cryptand/paraquat complexes[5a,15] and **3b•2a**. This angle is zero in **2a** (Figure 1a) and its other 2:1 cryptand complexes.[14] This big change in the angle presumably occurs in order to maximize the hydrogen-bonding between **3d** and **2a**; three of the four α-pyridinium hydrogens are H-bonded (**R**, **S**, **T**, and **U**). None of the β-pyridinium hydrogens are bound to the host's ethyleneoxy chains (see below, however), while in the other cryptand/paraquat complexes at least one β-pyridinium hydrogen is bound to the host's ether oxygen atoms directly or indirectly.[5a,14,15]

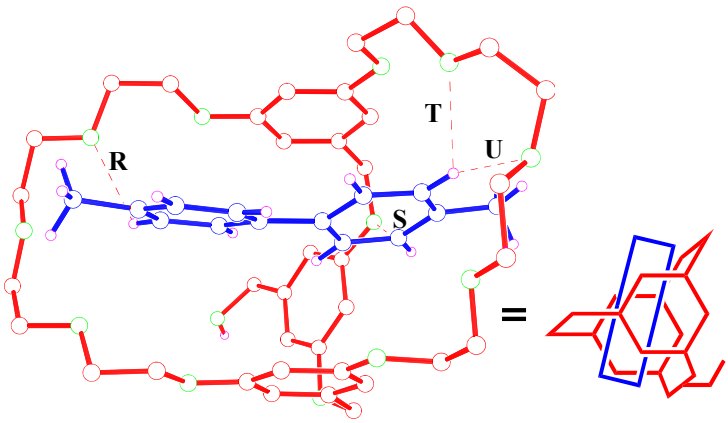

Figure 5. X-ray structure of **3d•2a**. Oxygens are green, hydrogens are magenta, **3d** is red, and **2a** is blue. An acetone molecule, two PF_6^- ions, and hydrogens except the ones on **2a** and the hydroxy group of **3d** have been omitted for clarity. Hydrogen-bond parameters: C···O distances (Å), H···O distances (Å), C-H···O angles (deg) **R**, 3.14, 2.54, 119; **S**, 3.11, 2.45, 123; **T**, 3.23, 2.26, 162; **U**, 3.14, 2.50, 122. Face-to-face π-stacking parameters: centroid-centroid distances (Å) 3.68, 4.28; ring plane/ring plane inclinations (deg): 7.9, 10.7. The centroid-centroid distance (Å) and dihedral angle (deg) between the pyridinium rings of **2a**: 4.27 and 21.3.

In the solid state, the complex is arranged linearly to form a supramolecular polycomplex by nesting each complex in the cleft of the next, resulting in an alternating pattern of orientation (Figure 6). The stablization forces between complex monomers are two hydrogen bonds between the oxygen atom of the hydroxyl group of the cryptand host of one complex and two β-pyridinium hydrogens on one side of the paraquat guest of the neighboring complex.

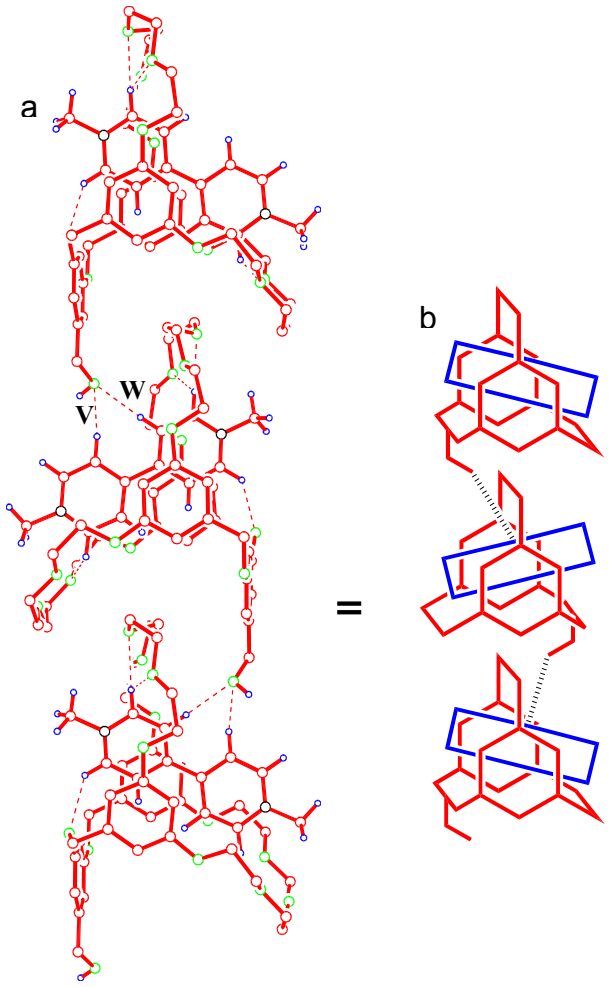

Figure 6. Ball-stick (a) and cartoon (b) representations of the **3d•2a** packing structure. (a) Hydrogens are blue, nitrogens are black, and oxygens are green. Three acetone molecules, six PF_6^- ions, and hydrogens except the ones on **2a** and hydroxy groups of **3d** have been omitted for clarity. Hydrogen-bonding parameters: C···O distances (Å), H···O distances (Å), C-H···O angles (deg) **V**, 3.26, 2.43, 141; **W**, 3.30, 2.31, 177. (b) **3d** molecules are red, and **2a** molecules are blue.

G. Solid State Structures of 3e and [2]Complex 3e•2a.

In the X-ray structure (Figure 7a) of hydroquinone-based cryptand **3e**, two crystallographically independent molecules were found. One is disordered and the other is not. An acetone molecule is located in the cavity of each molecule. The phenylene rings in both structures are almost parallel to each other with small dihedral angles of 5.0° and 5.1°. This is different from the crystal structure (Figure 3b) of pyridyl ester cryptand **3b**, in which the phenylene rings are twisted with an angle of 36°. The centroid-centroid distances of the phenylene rings of both structures are almost the same, 7.20 Å and 7.23 Å.

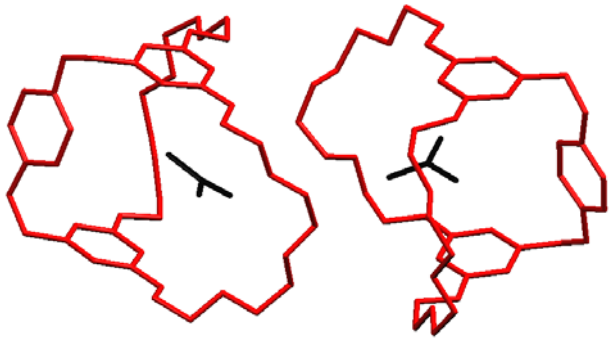

Figure 7. X-ray structures of **3e**. **3e** molecules are red and acetone molecules are black. Other solvent molecules and hydrogens have been omitted for clarity. The centroid-centroid distances (Å) and dihedral angles (deg) between the phenylene rings of the two **3e** molecules: 7.20 and 5.0 for the left one and 7.23 and 5.1 for the right one.

Bright yellow crystals of **3e•2a** are visually very nice, but they are not single and do not give clean diffraction patterns. Only a preliminary crystal structure was obtained (see Supporting Information). However, it is obvious that the complex between **3e** and **2a** has a 1:1 stoichiometry in the solid state and the guest **2a** is threaded into the cavity of the 32-crown-10 part of the cryptand host **3e**, similarly to complex **3d•2a**.

H. Mass Spectrometric Characterization of Cryptand Complexes.

The 1:1 stoichiometries of the complexes based on the four new cryptands and paraquat **2a** were confirmed by electrospray ionization mass spectrum (ESIMS). We observed two peaks for **3b•2a** using a solution of **3b** and **2a** in 4:1 acetonitrile:chloroform: *m*/*z* 1058 [**3b•2a** - PF_6]$^+$ (50%) and 457 [**3b•2a** - $2PF_6$]$^{2+}$ (100%) (Figure 8). The same peaks but with different relative intensities were found in methanol: *m*/*z* 1058 [**3b•2a** - PF_6]$^+$ (18%) and 457 [**3b•2a** - $2PF_6$]$^{2+}$ (20%) (base peak at *m*/*z* 186 corresponding to [**2a** - $2PF_6$]$^+$).

The following peaks were detected for **3c•2a** using a solution of **3c** and **2a** in methanol: *m*/*z* 1147 [**3c•2a**]$^+$ (0.5%), 1058 [**3c•2a** - HPF_6 + K + H_2O]$^+$ (2%), 1002 [**3c•2a** - PF_6]$^+$ (4%), and 429 [**3c•2a** - $2PF_6$]$^{2+}$ (2%) (base peak at *m*/*z* 331 corresponding to [**2a** - PF_6]$^+$).

Three peaks were observed for **3d•2a** using a solution of **3d** and **2a** in methanol: *m*/*z* 1031 [**3d•2a** - PF_6]$^+$ (6%), 927 [**3d•2a** - $2PF_6$ + K]$^+$ (2%), and 452 [**3d•2a** - $2PF_6$ + H_2O]$^{2+}$ (1%) (base peak at *m*/*z* 331 corresponding to [**2a** - PF_6]$^+$).

Two peaks were observed for **3e•2a** using a solution of **3e** and **2a** in 4:1 acetonitrile:chloroform: *m*/*z* 1001 [**3e•2a** - PF_6]$^+$ (14%) and 428 [**3e•2a** - $2PF_6$]$^{2+}$ (100%).

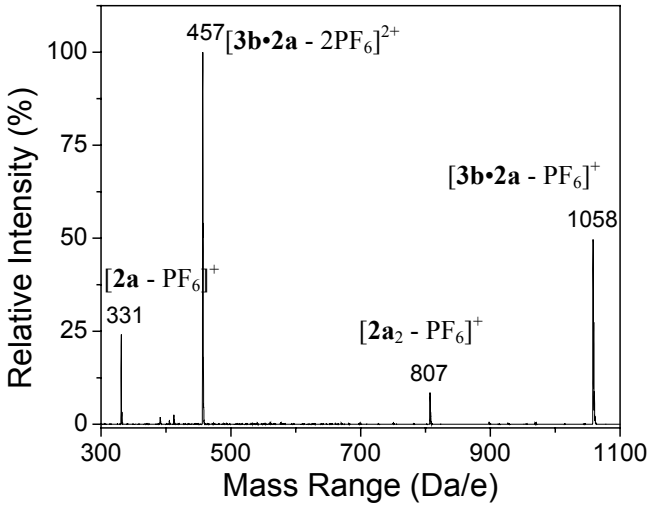

Figure 8. Electrospray mass spectrum of a solution of **3b** and **2a** in a mixture of acetonitrile and chloroform (4:1).

The very strong binding ability of pyridyl ester cryptand **3b** for paraquat derivatives was emphatically confirmed by FABMS of a solution of **3b** and **2b** (1:1 molar ratio) (Figure 9). The base peak at m/z = 1119 corresponds to [**3b•2b** - PF_6]$^+$; the next peak at m/z = 974 of 55% intensity corresponds to [**3b•2b** - $2PF_6$]$^+$, and the cryptand signal at m/z = 728 constitutes only 35% in intensity!! No any other pseudorotaxane has revealed such a preponderance of the complex in its mass spectrum to our knowledge.

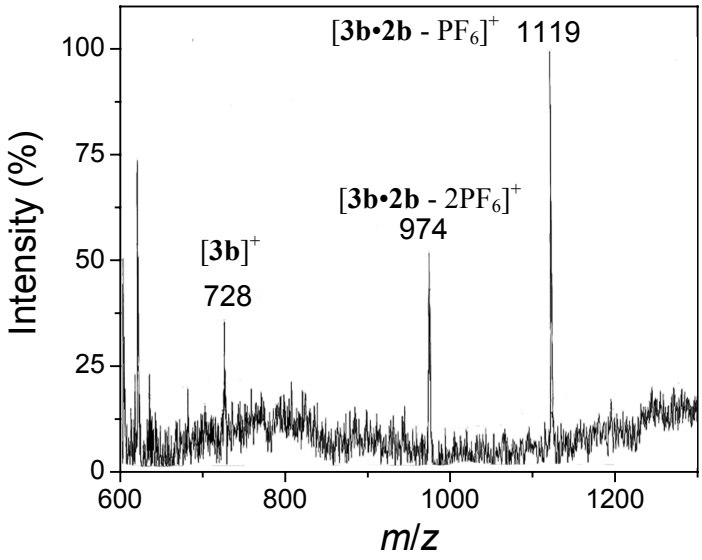

Figure 9. Fast-atom bombardment mass spectrum of an acetone solution of **2b** and **3b** (1:1 molar ratio). The matrix is GLY.

I. Electrostatic Potential Maps of Cryptand Hosts and Guest 2a at the AM1 Level.

Electrostatic potential maps (Figure 10) of **2a**, **3b**, **3c**, **3d**, and **3e** at the AM1 level were determined with the CAChe program. It is obvious that paraquat guest **2a** is very electron-poor, while the cryptand hosts have electron-rich cavities, so strong charge-transfer interactions can form between the cryptand host and paraquat guest when any of these cryptand hosts is put into acetone with **2a**. All hydrogens, including methyl hydrogens, on paraquat **2a** have very low electron density so they want to form hydrogen-bonds with electron-rich atoms, such as ether oxygen atoms and pyridyl nitrogen atoms, on the cryptand hosts. In solution some of these hydrogens can interact with solvent molecules and the rest with the host, resulting in 1:1 stoichiometry for these cryptand/paraquat complexes. In the solid state, no or not enough solvent molecules are available to interact with these acidic hydrogens so hydrogen bonds are provided by the hosts in 2:1 stoichiometry. This is probably the main reason for the formation of 2:1 complexes (**3a•2a•3a**, **3c•2a•3c**, and **3f•2a•3f**) between cryptand hosts and paraquat in the solid state. The pyridyl nitrogen atoms of **3b** and **3c** are electron-rich (Figures 10b and 10c), so they are good hydrogen-bonding acceptors for hydrogens on paraquat.

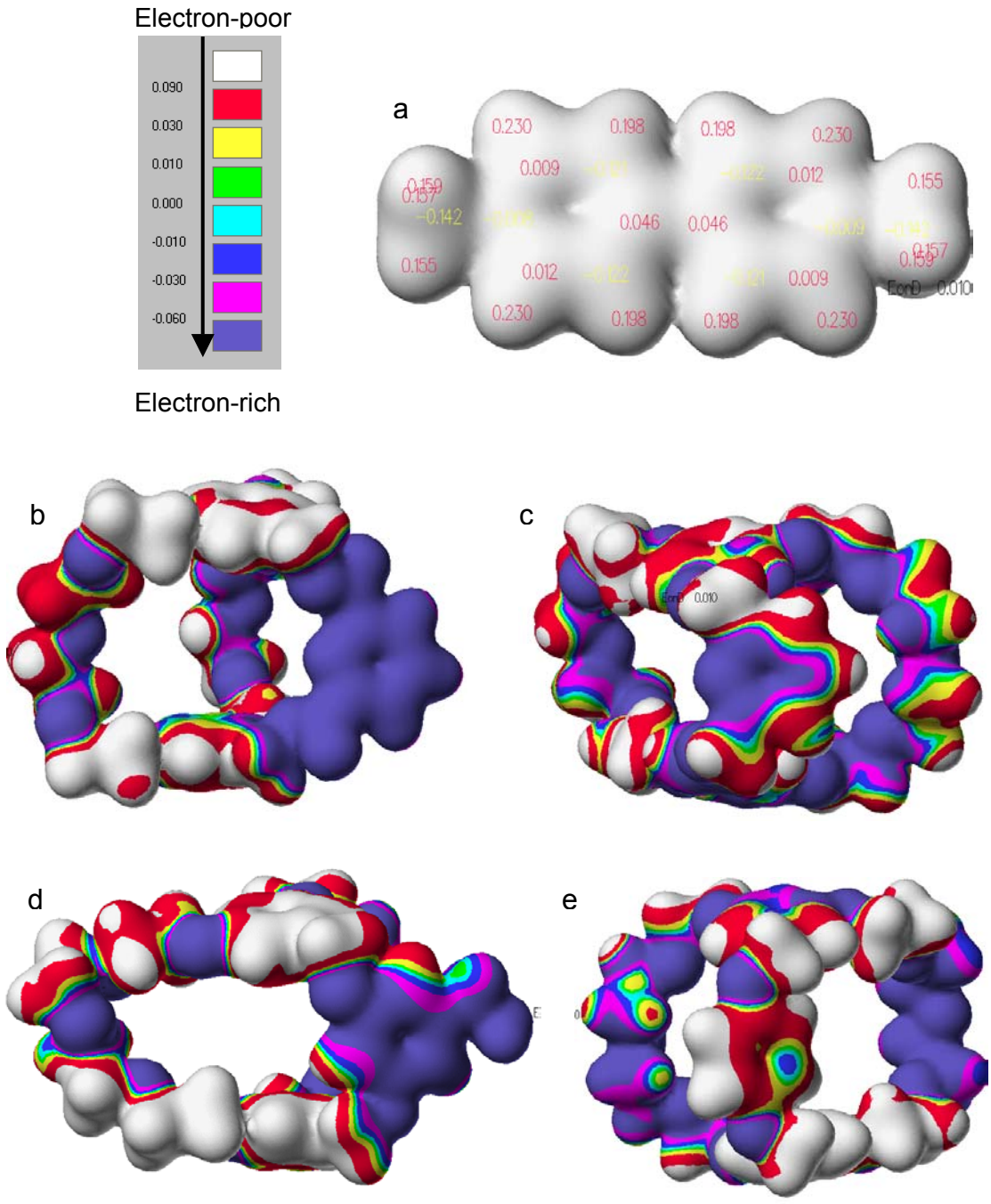

Figure 10. Electrostatic potential maps of **2a** (a), **3b** (b), **3c** (c), **3d** (d), and **3e** (e) at the AM1 level as determined with the CAChe program.

5.3. CONCLUSIONS

It has been demonstrated that bis(*m*-phenylene)-32-crown-10 based cryptands are powerful hosts for paraquat derivatives compared with the simple crown ether host. The significant improvement in complexation is the result of the combination of the preorganization of the cryptand hosts and the introduction of additional and optimized binding sites. Specifically, pyridyl ester cryptand **3b**, which has a pyridyl nitrogen atom located at a site occupied by either water or a PF_6 anion in analogous complexes, exhibited the highest association constant $K_a = 5.0 \times 10^6$ M^{-1} in acetone with paraquat, 9000 times greater than the crown ether system. These readily accessible cryptands are valuable host structures in the construction of larger supramolecular systems. Currently, we are focusing on these projects.

5.4. EXPERIMENTAL SECTION

General Procedures. Dimethylformamide (DMF) was distilled under reduced pressure. Other chemicals were reagent grade and used as received. All solvents were HPLC or GC grade. NMR solvents were bought from Cambridge Isotope Laboratories and used as received. The NMR spectra were recorded on a Varian Unity or Inova Instrument. Low-resolution electron impact mass spectroscopy (LREIMS) was carried out on VG-Quohro 4000 (direct probe inlet) Triple Quodrupole Mass Spectrometer. Low-resolution fast-atom bombardment mass spectroscopy (LRFABMS) and high-resolution fast-atom bombardment mass spectroscopy (HRFABMS) was carried out on HX110 Dual Focusing Mass Spectrometer using xenon gas for ionization. Low-resolution electrospray ionization mass spectroscopy (LRESIMS) of **3b•2a**, **3c•2a**, and **3d•2a** in methanol were performed by HT Laboratories of San Diego, CA. LRESIMS of **3b•2a** and **3e•2a** in 4:1 acetonitrile:chloroform were carried out on a local TSQ Finnigan LC/MS/MS instrument. Melting points were taken in capillary tubes and are uncorrected. Elemental analyses were performed by Atlantic Microlabs of Norcross, GA.

Complexation Studies by Proton NMR. All solutions were prepared as follows. Precisely weighed amounts of dried hosts and guests were added into separate screw cap

vials. The solvent was added with to-deliver volumetric pipets. Then specific volumes of each fresh solution were mixed to yield the desired concentrations. For example, in order to make three solutions, 0.500 mM **3e**/1.00 mM **2a,** 0.500 mM **3e**/3.00 mM **2a**, and 0.500 mM **3e**/5.00 mM **2a**, a 1.00 mM solution of **3e** was made first by adding 5.00 mL acetone-d_6 with a 5.00 mL to-deliver pipette into a screw cap vial containing 3.35 mg (0.00500 mmol) of **1**. Then 0.300 mL of this solution was added with a 0.300 mL to-deliver pipet to three vials that contained 0.300 mL of 2.00 mM, 0.300 mL of 6.00 mM, and 0.300 mL of 10.0 mM of **2a** separately. ^{1}H NMR data were collected on a temperature controlled spectrometer. Acetone-d_6 was chosen as the NMR solvent because all compounds used here have relatively good solubilities in it. Error bars were calculated based on a 0.05 mg deviation in weight, a 0.001 ppm deviation in chemical shift on proton NMR spectra, and a $\pm$2% deviation in fractional complexation (Δ/Δ_0). Standard errors in both the intercept and slope coefficients based on regression were used to determine errors in association constants.

Bis(1,3,5-phenylene)di(1',4',7',10',13'-pentaoxatridecyl)[2'',6''-di(methyleneoxycarbonyl)pyridine] (unoptimized synthesis of 3b). To a stirred solution of 1 mL pyridine and 200 mL CH_3CN under N_2 **1b**[10] (0.50 g, 0.84 mmol) in 25 mL of CH_3CN was added dropwise at approximately the same rate as 0.17 g (0.84 mmol) of 2,6-pyridinedicarbonyl dichloride in 25 mL CH_3CN. The reaction mixture was stirred for 1 h after addition of the reactants. The solvent was removed by rotoevaporation to give a white solid, which was dissolved in 40 mL of $CHCl_3$, and washed with water (3 × 40 mL) and 5% $NaHCO_3$ (3 × 40 mL). The organic layer was evaporated to dryness using a rotoevaporator, producing a yellow viscous oil. Column chromatography (silica gel, 9:1 chloroform:acetone) was employed to isolate **3b**. Recrystallization from EtOAc-hexane provided 20 mg (3.3%, which is low for this kind of reaction; a higher yield is expected now because we made a **3b** derivative in 21% yield[15b]) of **3b**, mp 153.5–155.3 °C. ^{1}H NMR (400 MHz, $CDCl_3$, 22 °C) δ (ppm): 8.37 (d, 2H J = 7.8 Hz), 8.05 (t, 1H, J = 7.8 Hz), 6.56 (d, 4H, J = 2.1 Hz), 6.47 (t, 2H, J = 2.1 Hz), 5.33 (s, 4H), 3.94 (m, 8H), 3.76 (m, 8H), and 3.65 (m, 16H). ^{13}C NMR (100 MHz, $CDCl_3$, 22 °C) δ (ppm): 164.880, 160.033, 148.252, 138.201, 137.245, 128.150, 106.325, 102.168, 70.960, 70.755, 69.640,

67.630, 67.539. Anal. calcd for $C_{37}H_{45}O_{14}N$: C 61.07, H 6.23, N 1.92; found: C 61.16, H 6.29, N 1.97. LRFABMS (NBA) *m/z* 728 $[M + H]^+$, 750 $[M + Na]^+$, 766 $[M + K]^+$; HRFABMS (NBA/PEG) *m/z* calcd for $[M + H]^+$ $C_{37}H_{46}O_{14}N$, 728.2918, found 728.2888, error 4.1 ppm.

Bis-(1,3,5-phenylene)di(1',4',7',10',13'-pentaoxatridecyl)(2'',6''-dioxymethylenepyridine) (3c). A solution of 700 mg (1.23 mmol) of **1c**[5a] and 326 mg (1.46 mmol) of 2,6-bis(bromomethyl)pyridine in 30 mL DMF was added at 0.75 mL/h into a suspension containing 2.07 g (15.0 mmol) of K_2CO_3 and 5.00 mg of $(n\text{-Bu})_4NI$ in 400 mL DMF under N_2 at 110 °C. After addition, the reaction mixture was stirred at 110 °C for 10 days, cooled and rotoevaporated. The residue was treated with $CHCl_3$ and filtered. Removal of $CHCl_3$ afforded a crude product that was purified by flash column chromatography (Et_2O increasing to EtOAc) to give 340 mg (41%) of **3c**, a pale yellow oil. ^{1}H NMR (400 MHz, $CDCl_3$, 22 °C) δ (ppm): 7.75 (t, 1H, *J* = 7.8 Hz), 7.37 (d, 2H, *J* = 7.8 Hz), 6.12 (t, 2H, *J* = 2.1 Hz), 6.07 (d, 4H, *J* = 2.1 Hz), 5.21 (s, 4H), 3.91 (s, 8H), 3.73 (t, 8H, *J* = 4.4 Hz), and 3.62 (s, 16H). ^{1}H NMR (400 MHz, CD_3COCD_3, 22 °C) δ (ppm): 7.84 (t, 1H, *J* = 7.8 Hz), 7.47 (d, 2H, *J* = 7.8 Hz), 6.12 (d, 4H, *J* = 2.1 Hz), 6.06 (t, 2H, *J* = 2.1 Hz), 5.19 (s, 4H), 3.94 (t, 8H, *J* = 4.4 Hz), 3.66 (t, 8H, *J* = 4.4 Hz), and 3.52 (m, 16H). LREIMS *m/z* 671 $[M + H]^+$, 672 $[M]^+$; HRFABMS (NBA/PEG) *m/z* calcd for $[M + H]^+$ $C_{35}H_{46}O_{12}N$, 672.3020; found 672.2991, error 4.3 ppm.

Synthesis of Bis(1,3,5-phenylene)di(1',4',7',10',13'-pentaoxatridecyl)[3'',5''-di(methyleneoxy)benzyl alcohol] (3d). A solution of 0.66 g (0.91 mmol) of **1e**[10] and 0.13 g (0.90 mmol) of 3,5-dihydroxybenzyl alcohol in 40 mL of DMF was added at 0.75 mL/h to a suspension containing K_2CO_3 (1.7 g, 12 mmol) and TBAI (5.00 mg) in 400 mL of DMF at 110 °C. After complete addition, the mixture was stirred at 110 °C for 5 days, evaporated to remove DMF, treated with dichloromethane, and filtered. Removal of dichloromethane afforded a crude product, which was purified by flash column chromatography using ethyl acetate:methanol (9:1) to afford pure **3d** as a white solid (0.27 g, 42%). mp 120.3-122.2 °C. ^{1}H NMR (400 MHz, $CDCl_3$, 22 °C) δ (ppm): 6.63 (4H, d, *J* = 2.0 Hz), 6.32 (2H, t, *J* = 2.0 Hz), 6.28 (2H, d, *J* = 2.0 Hz), 6.09 (1H, t, *J* = 2.0 Hz), 5.01 (4H, s), 4.63 (2H, d, *J* = 6.2 Hz), 3.94 (8H, m), 3.81 (8H, m), 3.65 (16H, s), and

2.01 (1H, t, J = 6.2 Hz). LRFABMS (NBA) *m/z* 723.4 $[M + Na]^+$, 700.3 $[M]^+$, 683.3 $[M-OH]^+$; HRFABMS (NBA/PEG) *m/z* calcd for $[M]^+$ $C_{37}H_{48}O_{13}$, 700.3095, found 700.3088, error 0.9 ppm.

Synthesis of Bis(1,3,5-phenylene)di(1',4',7',10',13'-pentaoxatridecyl)[1'',4''-di(methyleneoxy)benzene] (3e). A solution of 360 mg (0.500 mmol) of **1e** and 50.0 mg (0.500 mmol) of hydroquinone in 40 mL DMF was added via a syringe pump at 1.00 mL/h into a suspension containing 3.20 (23.0 mmol) g of potassium carbonate and 2.00 mg of tetrabutylammonium iodide in 150 mL DMF at 110 °C. After complete addition, the reaction mixture was stirred at 110 °C for further 5 days. The cooled mixture was evaporated to remove DMF, treated with chloroform, and filtered. Removal of chloroform afforded a crude product. The crude product was purified by flash column chromatography eluting with ethyl acetate to afford **3e** as a white solid, 142 mg (42%). mp 98.1.5-99.0 °C. ^{1}H NMR (400 MHz, $CDCl_3$, 22 °C) δ (ppm): 6.67 (4H, s), 6.52 (4H, d, J = 2.4 Hz), 6.41 (2H, t, J = 2.4 Hz), 5.04 (4H, s), 4.07 (8H, t, J = 4.2 Hz), 3.81 (8H, t, J = 4.2 Hz), and 3.68 (16H, s). LRFABMS (NBA) *m/z* 671.3 $[M + H]^+$; HRFABMS (NBA/PEG) *m/z* calcd for $[M]^+$ $C_{36}H_{47}O_{12}$, 670.2989, found 670.2976, error 2.0 ppm.

Determination of the association constant ($K_{a,3b•2a}$) for 3b•2a. The association constant ($K_{a,3b•2a}$) for **3b•2a** was determined using a competitive NMR method recently developed by Smith Group.[12] 1,1'-Ethylene-2,2'-dipyridinium bis(hexafluorophosphate) ("diquat" **7**) was used as the reference guest. In a 0.670 mM equimolar acetone-d_6 solution of reference host **3a**, cryptand **3b**, and guest **7**, the concentration of complexed **3a**, $[\mathbf{3a}]_c$, was 0.174 mM. $K_{a,3b•7}$ was thus determined to be 3.30 (± 0.66) × 10^5 M^{-1}. The error is based on errors of $[\mathbf{3a}]_c$ and $K_{a,3a•7}$, which was determined using the method discussed below for the determination of $K_{a,3c•2a}$, $K_{a,3d•2a}$, and $K_{a,3e•2a}$. Then, in a 0.500 mM equimolar acetone-d_6 solution of guest **2a**, cryptand host **3b**, and **7**, the concentration of complexed reference guest **7**, $[\mathbf{7}]_c$, was 0.102 mM. $K_{a,3b•2a}$ was thus determined to be 5.0 (± 2.0) × 10^6 M^{-1}. The error is based on errors of $[\mathbf{7}]_c$ and $K_{a,3b•7}$.

Determination of association constants ($K_{a,3c•2a}$, $K_{a,3d•2a}$, and $K_{a,3e•2a}$) for 3c•2a, 3d•2a, and 3e•2a. $K_{a,3c•2a}$, $K_{a,3d•2a}$, and $K_{a,3e•2a}$ were determined in the same way. Here the determination of $K_{a,3c•2a}$ is given as an example. ^{1}H NMR characterizations were done

on solutions with constant [**3c**] and varied [**2a**]. Based on these NMR data, $\Delta_{0,\mathbf{3c}}$, the difference in δ values for H_1 of **3c** in the uncomplexed and fully complexed species, was determined by the extrapolation of a plot of $\Delta = \delta - \delta_u$ vs. $1/[\mathbf{2a}]_0$ in the high initial concentration range of **2a**. Then $K_{a,\mathbf{3c•2a}}$ was calculated from $K_{a,\mathbf{3c•2a}} = (\Delta_{\mathbf{3c}}/\Delta_{0,\mathbf{3c}})/\{1 - (\Delta_{\mathbf{3c}}/\Delta_{0,\mathbf{3c}})\}\{[\mathbf{2a}]_0 - (\Delta_{\mathbf{3c}}/\Delta_{0,\mathbf{3c}})[\mathbf{3c}]_0\}$. The $\Delta_{0,\mathbf{3}}$ values for **3c•2a**, **3d•2a**, and **3e•2a** were determined to be 0.599 ppm, 0.604 ppm, and 0.701 ppm in acetone, respectively. The error of $K_{a,\mathbf{3c•2a}}$ is based on experimentally observed 2% variation in Δ/Δ_0 values over the range 0.2 - 0.8.

X-ray analysis of 2a. Colorless crystals of **2a** were grown by vapor diffusion of pentane into its acetone solution. X-Ray diffraction experiment was carried out on a Bruker Apex CCD diffractometer equipped with MoK_α radiation (λ = 0.71073 Å) and a graphite monochromator. Data were collected from θ = 2.38º to θ = 24.99º by using phi and omega scans. SADABS[16] absorption corrections were applied. The structure was solved by direct methods and refined by full-matrix least squares procedure on F^2 using the SHELXTL.[17] Non-hydrogen atoms were refined with anisotropic displacement coefficients, and hydrogen atoms were treated as idealized contributions. Crystal data: rod, colorless, 0.50 × 0.10 × 0.10 mm^3, $C_{12}H_{14}F_{12}N_2P_2$, FW 476.19, orthorhombic, space group *P*nma, a = 14.4612(16)**,** b = 11.6741(13), c = 10.6275(11) Å, $\alpha = \beta = \gamma$ = 90º, V = 1794.2(3) $Å^3$, Z = 4, D_c = 1.763 g cm^{-3}, T = 218 K, μ = 3.62 cm^{-1}, 10268 measured reflections, 1664 independent reflections, 139 parameters, $F(000)$ = 752, R_1 = 0.0757, wR_2 = 0.1816 (all data), R_1 = 0.0674, wR_2 = 0.1753 [I > 2σ(I)], max. residual density 0.498 e•$Å^{-3}$, max./min. transmission 0.9647/0.8397, and goodness-of-fit (F^2) = 1.113.

X-ray analysis of 3b. Colorless crystals of **3b** were grown by slow evaporation of a 9:1 chloroform:acetone solution of **3b**. X-Ray diffraction data were collected on a Siemens Bruker P4 diffractometer by the omega scan method in a range $2.0^o \leq \theta \leq 25.0^o$. SADABS absorption corrections were applied. The structure was solved by direct methods and refined by full-matrix least squares procedure on F^2 using the SHELXTL. Non-hydrogen atoms were refined with anisotropic displacement coefficients, and hydrogen atoms were treated as idealized contributions. Crystal data: block, colorless, 0.60 × 0.40 × 0.30 mm^3, $C_{37}H_{45}NO_{14}$, FW 727.74, Monoclinic, space group C_2/c, a =

17.688(3), b = 11.184(2), c = 18.034(5) Å, β = 96.030(14)°, V = 3547.9(18) Å^3, Z = 4, D_c = 1.362 g cm^{-3}, T = 241K, μ = 1. 05 cm^{-1}, 3555 measured reflections, 2931 independent reflections [R(int) = 0.0464], 236 parameters, F(000) = 1544, R_1 = 0.1490, wR_2 = 0.2873 (all data), R_1 = 0.0867, wR_2 = 0.2060 [$I > 2\sigma(I)$], maximum residual density 0.436 e•Å^{-3}, and goodness-of-fit (F^2) = 1.573.

X-ray analysis of 3b•2a. Bright yellow crystals of **3b•2a** were grown by vapor diffusion of pentane into an acetone solution of **3b** and **2a** (1:1). X-Ray diffraction data were collected on an Oxford Diffraction XCalibur2™ diffractometer equipped with the Enhance X-ray Source™ (MoKα radiation; λ = 0.71073 Å) and a Sapphire 2™ CCD detector by the phi and omega scan method in a range 1.06$^o \le \theta \le$ 27.50^o. The structure was solved by the direct methods using SIR[18] and refined by full-matrix least squares using Crystals.[19] Crystal data: prism, yellow, 0.38 × 0.20 × 0.12 mm^3, $C_{58}H_{77}F_{12}N_3O_{17}P_2$, FW 1378.18, monoclinic, space group $P2_1/c$, a = 13.9159(17), b = 21.217(2), c = 21.768(2) Å, β = 95.423(9)°, V = 6398.3(12) Å^3, Z = 4, D_c = 1.431 g cm^{-3}, T = 100K, μ = 1.73 cm^{-1}, 82374 measured reflections, 20876 independent reflections [R(int) = 0.03], 829 parameters, F(000) = 2880.000, R_1 = 0.1950, wR_2 = 0.1524 (all data), R_1 = 0.0618, wR_2 = 0.1223 [$I > 2\sigma(I)$], maximum residual density 1.32 e•Å^{-3}, and goodness-of-fit (F^2) = 0.9244.

X-ray analysis of 3c•2a•3c. Yellow crystals of **3c•2a•3c** were grown by vapor diffusion of pentane into a 1:1 acetonitrile:acetone solution of **3c** and **2a** (1:2 molar ratio). X-Ray diffraction data were collected on a Bruker Apex CCD diffractometer equipped with MoK$_\alpha$ radiation (λ = 0.71073 Å) and a graphite monochromator by the phi and omega scan method in a range 1.06$^o \le \theta \le$ 28.28^o. SADABS absorption corrections were applied. The structure was solved by direct methods and refined by full-matrix least squares procedure on F^2 using the SHELXTL. Non-hydrogen atoms were refined with anisotropic displacement coefficients, and hydrogen atoms were treated as idealized contributions. Besides the main **3c•2a•3c** molecule in the crystal structure there are two acetonitrile, water and acetone solvent molecules. The acetone molecule is disordered around a center of symmetry and was treated by SQUEEZE.[20] Correction of the X-ray data by SQUEEZE (38 *e*/cell) was close to the required values (32 *e*/cell). Crystal data:

block, yellow, 0.45 × 0.30 × 0.20 mm^3, $C_{46.50}H_{63}F_6N_4O_{13.50}P$, FW 1038.98, triclinic, space group *P*-1, a = 10.3991(6), b = 13.6159(8), c = 19.3423(12) Å, α = 87.7590(10)°, β = 82.5240(10)°, γ = 72.6750(10)°, V = 2592.3(3) $Å^3$, Z = 2, D_c = 1.331 g cm^{-3}, T = 100K, μ = 1.40 cm^{-1}, 19230 measured reflections, 11808 independent reflections [R(int) = 0.0229], 622 parameters, F(000) = 1094, R_1 = 0.0954, wR_2 = 0.2265 (all data), R_1 = 0.0710, wR_2 = 0.2084 [$I > 2\sigma(I)$], maximum residual density 0.816 e•$Å^{-3}$, and goodness-of-fit (F^2) = 1.067.

X-ray analysis of 3d•2a. Bright yellow crystals of **3d•2a** were grown by vapor diffusion of pentane into an acetone solution of **3d** and **2a** (1:1). X-ray diffraction data were collected in a range $2.5^o \leq \theta \leq 25.0^o$ on a Nonius KappaCCD diffractometer equipped with MoKα radiation (λ = 0.71073 Å), a graphite monochromator, and an Oxford Cryostream chiller. The structure was solved by the direct method SIR and refined by full-matrix least squares using Crystals. Nonhydrogen atoms were treated anisotropically and hydrogen atoms were placed in calculated positions. 9851 reflections were used in refinements by full-matrix least-squares on F^2. Crystal data: Prism, yellow, 0.25 × 0.20 × 0.12 mm^3, $C_{52}H_{68}F_{12}N_2O_{14}P_2$, FW 1235.04, monoclinic, space group $P2_1/c$, a = 11.871(3), b = 23.066(5), c = 20.450(6) Å, β = 90.307(8)º, V = 5599.5(25) $Å^3$, Z = 4, D_c = 1.465 g cm^{-3}, T = 100 K, μ = 1.84 cm^{-1}, 68453 measured reflections, 9851 independent reflections, 739 parameters, F(000) = 2576, R_1 = 0.1427, wR_2 = 0.1674 (all data), R_1 = 0.0588, wR_2 = 0.0891 [$I > 4\sigma(I)$], max. residual density 0.96 e•$Å^{-3}$, max./min. transmission 0.979/0.940, and goodness-of-fit (F^2) = 1.1035.

X-ray analysis of 3e. Colorless crystals of **3e** were grown by slow evaporation of an acetone solution of **3e** at room temperature. The chosen crystal was mounted on a nylon CryoLoop™ (Hampton Research) with Krytox® Oil (DuPont) and centered on the goniometer of a Oxford Diffraction XCalibur2™ diffractometer equipped with a Sapphire 2™ CCD detector. The data collection routine, unit cell refinement, and data processing were carried out with the program CrysAlis.[21] The structure was solved by direct methods and refined using the SHELXTL program package. The asymmetric unit of the structure comprises two crystallographically independent molecules of **3e**, three acetone molecules, and 2.93 water molecules. Successful refinement of the structure was

plagued by disorder in one arm of a **3e** molecule, the acetone molecules, and additional residual electron density that was modeled as water. The arm of the **3e** molecule was modeled as adopting two conformations that refined to occupancies of 0.528(3) and 0.472(3). The disordered acetone was modeled as adopting two conformations with occupancies of 0.578(7) and 0.422(7). Four strong residual electron density peaks, all within 2.7-3.0 Å of other oxygen atoms were presumed to be the oxygen atoms of water molecules. Two of these Fourier peaks were refined as fully occupied oxygen sites. The remaining two Fourier peaks could not have full occupancy due to their close proximity to the disordered **3e** arm, and refined to occupancies 0.432(9) and 0.50(1). The size of the anisotropic thermal parameters in the remaining two acetone molecules as well as the prevalence of residual electron density peaks near the molecules suggest additional disorder which was not modeled successfully. The final refinement involved an anisotropic model for all non-hydrogen atoms and a riding model for all hydrogen atoms. A total of six hydrogen atoms from the disordered **3e** molecule, three from the disordered acetone and the hydrogen atoms of the water molecules were all absent from the model. Crystal data: plate, colorless, 0.48 × 0.24 × 0.085 mm^3, $2C_{36}H_{46}O_{12}\bullet 3C_3H_6O\bullet 2.93H_2O$, FW 1568.48, triclinic, space group *P*-1, a = 10.7938(13)**,** b = 20.2260(19), c = 21.431(2) Å; α = 63.096(9)º, β = 83.239(10)º, γ = 84.292(9)º; V = 4137.6(7) $Å^3$, Z = 2, D_c = 1.259 g cm^{-3}, T = 100 K, μ = 0.96 cm^{-1}, 22982 measured reflections, 14609 independent reflections[R(int) = 0.0234], 1100 parameters, $F(000)$ = 1683, R_1 = 0.0889, wR_2 = 0.2076 (all data), R_1 = 0.0699, wR_2 = 0.1926 [$I > 2\sigma(I)$], and GooF (F^2) = 1.109.

Calculations of electrostatic potential maps of 2a, 3b, 3c, 3d, and 3e at AM1 level with the CAChe program. CAChe WorkSystem Pro Version 6.1 was used in the calculations of electrostatic potential maps of **2a**, **3b**, **3c**, **3d**, and **3e**. The structures of these compounds were inputted from their individual crystal structures (**2a**, **3b**, and **3e**) or paraquat complex crystal structures (**3c•2a•3c** and **3d•2a**). Then their electrostatic potential maps at AM1 level were calculated under AM1 geometry using the AM1 wavefunction

5.5. ACKNOWLEDGEMENTS

This research was supported by the National Science Foundation (DMR0097126) and the American Chemical Society Petroleum Research Fund (40223-AC7). We also thank NSF (Grant CHE-0131128) for funding of the purchase of the Oxford Diffraction Xcalibur2 single crystal diffractometer. We thank Professor Richard D. Gandour at Virginia Tech for helpful discussion on calculations of electrostatic potential maps of cryptands and paraquat with the CACHe program.

5.6. SUPPORTING INFORMATION

*The preliminary crystal structure of **3e•2a***

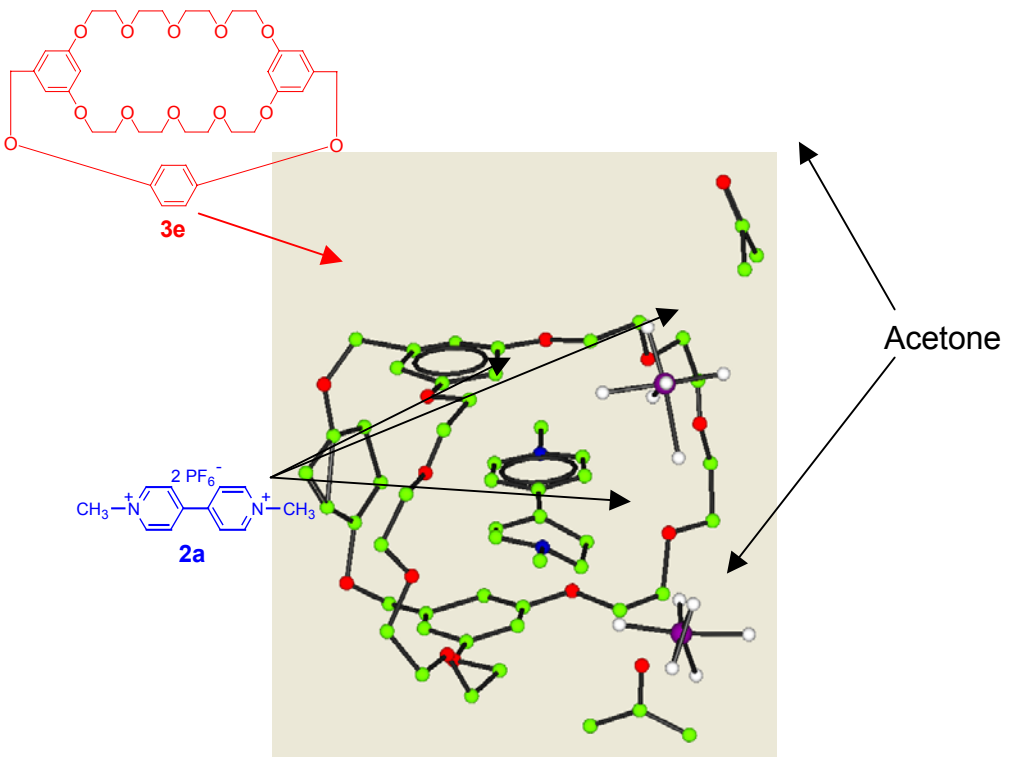

Bright yellow crystals of **3e•2a** were grown by vapor diffusion of pentane into an acetone solution of **2a** with excess **3e**. The structure was solved by the direct method SIR[S1] in Crystals.[21] Data were collected in a range $1.06^{o} \leq \theta \leq 27.50^{o}$ on an Oxford

Diffraction XCalibur2™ diffractometer equipped with the Enhance X-ray Source™ (MoKα radiation; λ = 0.71073 Å) and a Sapphire 2™ CCD detector by the phi and omega scan method.

S1. Altomare, A.; Cascarano, G.; Giacovazzo, C.; Guagliardi, A. *J. Appl. Cryst.* **1993**, *26*, 343-350.

S2. Watkin, D. J.; Prout, C. K.; Carruthers, J. R.; Betteridge, P. W.; Cooper, R. I. CRYSTALS **2000**, Issue 11. Chemical Crystallography Laboratory, University of Oxford, Oxford.

*Electrospray mass spectrum of a solution of **3b** and **2a** in methanol*

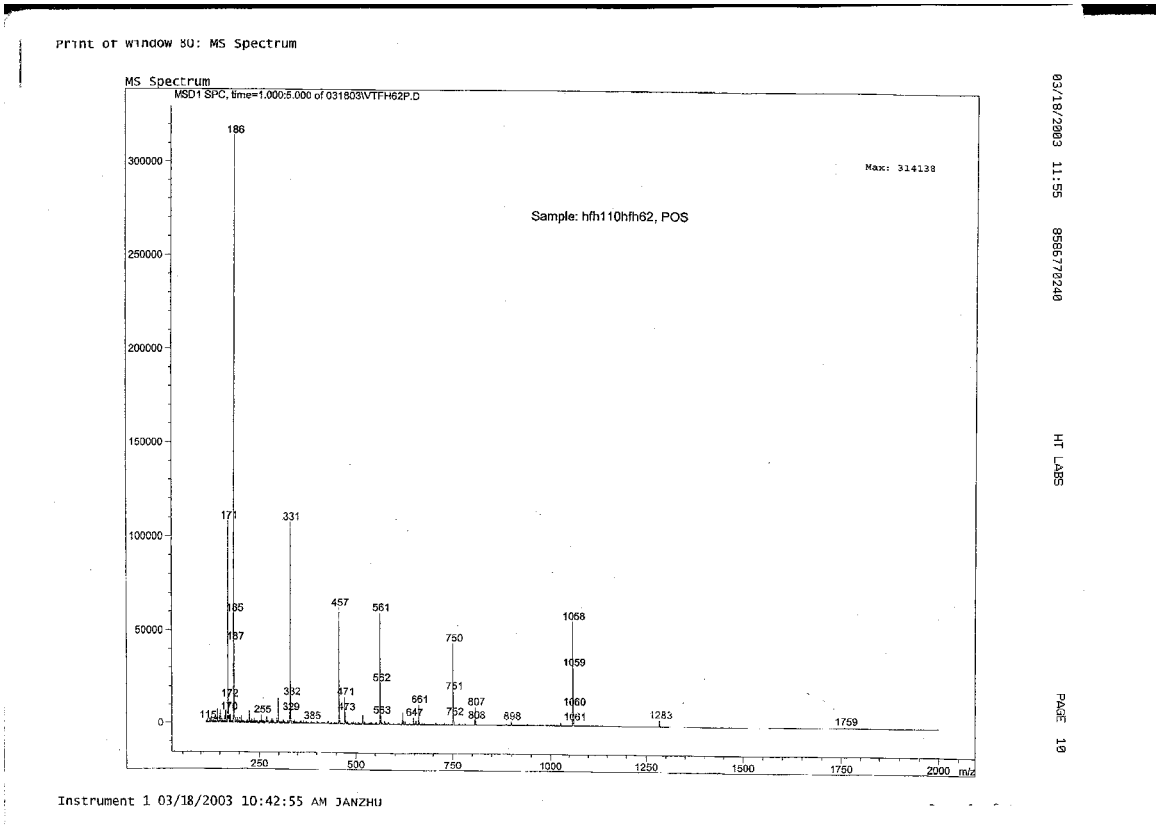

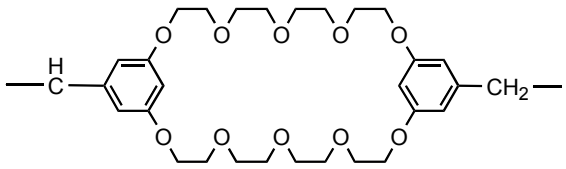

S1

$C_{30}H_{41}O_{10}$

Assignments of main peaks: *m/z* 1058 [**3b•2a** - PF_6]$^+$, 898 [**3b•2a** - $2PF_6$ - CH_3]$^+$, 807 [**2a**$_2$ - PF_6]$^+$, 750 [**3b** + Na]$^+$, 561 [**S1**]$^+$, 457 [**3b•2a** - $2PF_6$]$^{2+}$, 331 [**2a** - PF_6]$^+$, 186 [**2a** - $2PF_6$]$^+$, and 171 [**2a** - $2PF_6$ - CH_3]$^+$.

*Electrospray mass spectrum of a solution of **3c** and **2a** in methanol*

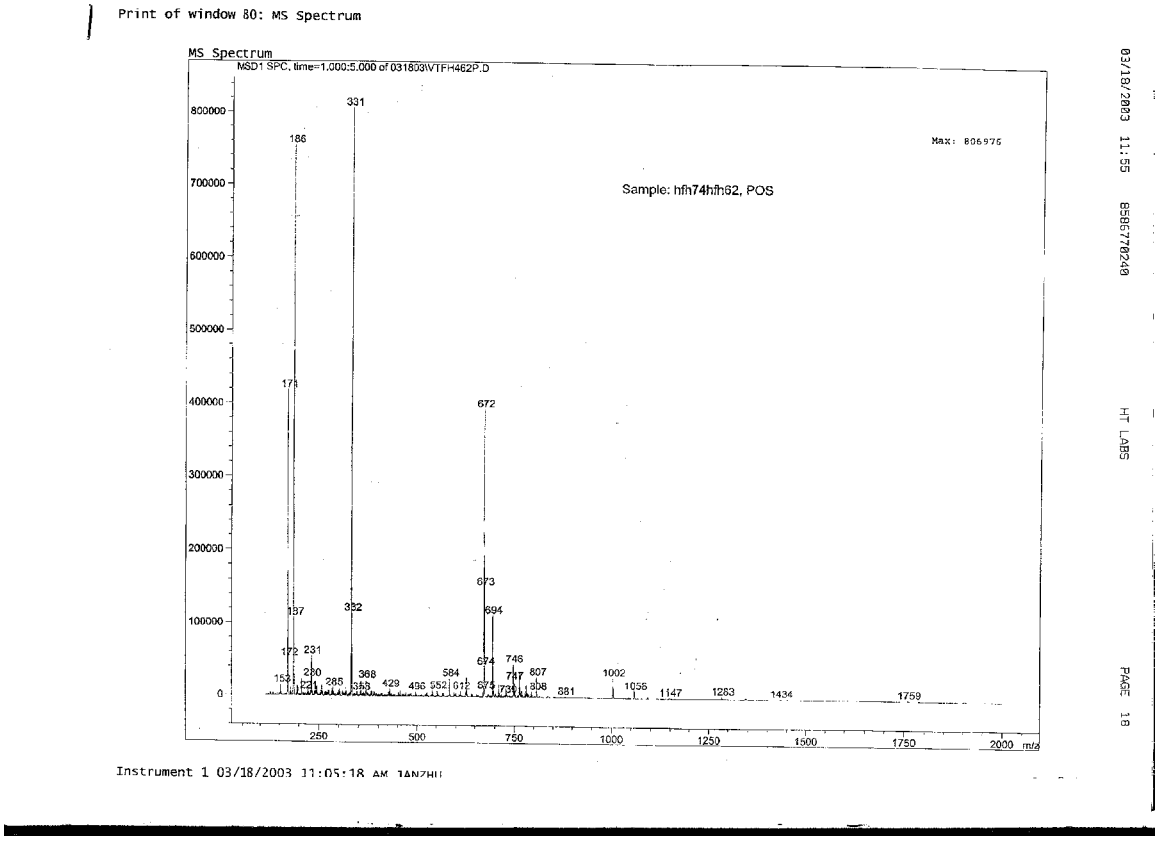

Assignments of main peaks: *m/z* 1147 [**3c•2a**]$^+$, 1058 [**3c•2a** - HPF_6 + K + H_2O]$^+$, 1002 [**3c•2a** - PF_6]$^+$, 807 [**2a**$_2$ - PF_6]$^+$, 694 [**3c** + Na]$^+$, 672 [**3c** + H]$^+$, 429 [**3c•2a** - $2PF_6$]$^{2+}$, 331 [**2a** - PF_6]$^+$, 186 [**2a** - $2PF_6$]$^+$, and 171 [**2a** - $2PF_6$ - CH_3]$^+$.

*Electrospray mass spectrum of a solution of **3d** and **2a** in methanol*

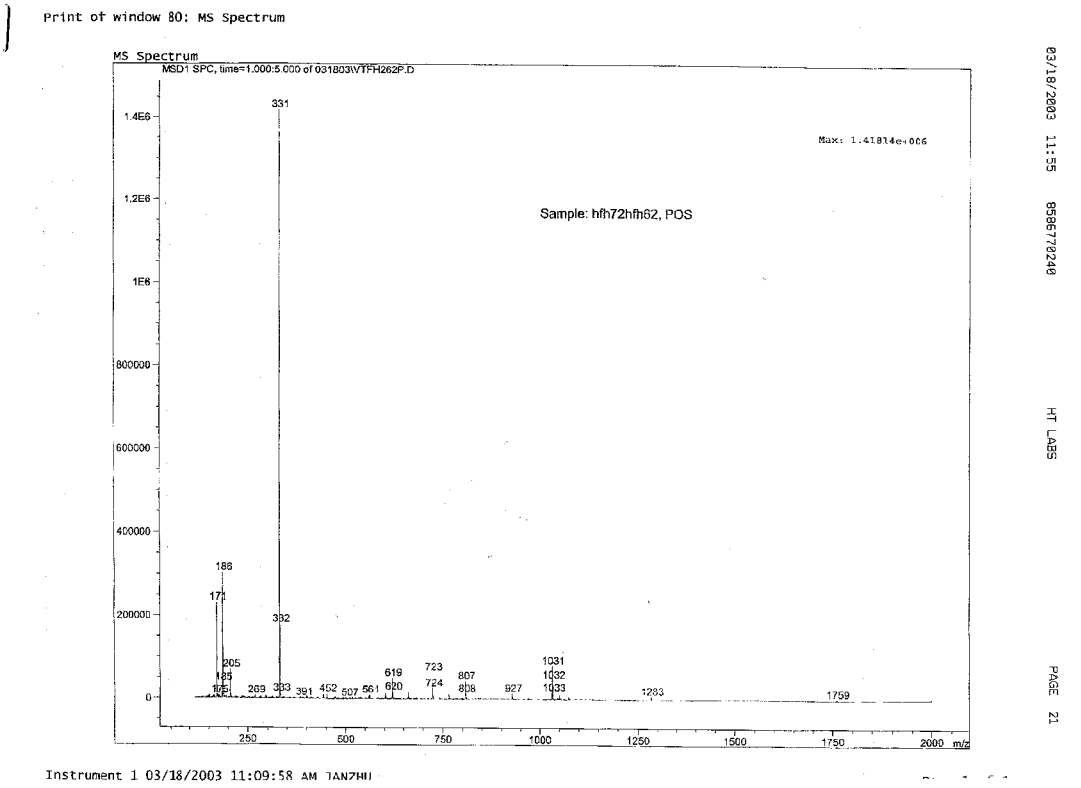

Assignments of main peaks: *m/z* 1031 [**3d•2a** - PF_6]$^+$, 927 [**3d•2a** - $2PF_6$ + K]$^+$, 807 [$\mathbf{2a}_2$ - PF_6]$^+$, 723 [**3d** + Na]$^+$, 619 [**S1** + K + H_2O]$^+$, 561 [**S1**]$^+$, 452 [**3d•2a** - $2PF_6$ + H_2O]$^{2+}$, 331 [**2a** - PF_6]$^+$, 186 [**2a** - $2PF_6$]$^+$, and 171 [**2a** - $2PF_6$ - CH_3]$^+$.

*Electrospray mass spectrum of a solution of **3e** and **2a** in a mixture of acetonitrile and chloroform (4:1)*

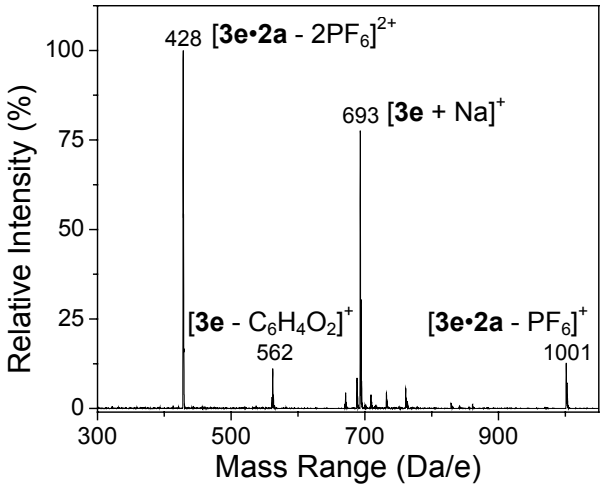

REFERENCES

1. (a) Ducharme, Y.; Wuest, J. D. *J. Org. Chem.* **1988**, *53*, 5789-5791. (b) Kato, T.; Fréchet, J. M. J. *J. Am. Chem. Soc.* **1989**, *111*, 8533-8534. (c) Hilger, C.; Dräger, M.; Stadler, R. *Macromolecules* **1992**, *25*, 2498-2501. (d) Chang, Y.-L.; West, M.-A.; Fowler, F. W.; Lauher, J. W. *J. Am. Chem. Soc.* **1993**, *115*, 5991-6000. (e) Wilson, L. M. *Macromolecules* **1994**, *27*, 6683-6686. (f) Pourcain, C. B. St.; Griffin, A. C. *Macromolecules* **1995**, *28*, 4116-4121. (g) Lehn, J.-M. *Supramolecular Chemistry* VCH: Weinheim, **1995**, pp 139-197.
2. (a) Sijbesma, R. P.; Beijer, F. H.; Brunsveld, L.; Folmer, B. J. B.; Hirshberg, J. H. K. K.; Lange, R. F. M.; Lowe, J. K. L.; Meijer, E. W. *Science* **1997**, *278*, 1601-1604. (b) Sijbesma, R. P.; Meijer, E. W. *Chem. Commun.* **2003**, 5-168. (c) Ojelund, K.; Loontjens, T.; Steeman, P.; Palmans, A.; Maurer, F. *Macromol. Chem. Phys.* **2003**, *204*, 52-60.
3. (a) Allwood, B. L.; Shahriari-Zavareh, H.; Stoddart, J. F.; Williams, D. J. *J. Chem.*

Soc., Chem. Commun. **1987**, 1058-1061. (b) Allwood, B. L.; Spencer, N.; Shahriari-Zavareh, H.; Stoddart, J. F.; Williams, D. J. *J. Chem. Soc., Chem. Commun.* **1987**, *14*, 1064-1066. (c) Ashton, P. R.; Slawin, A. M. Z.; Spencer, N.; Stoddart, J. F.; Williams, D. J. *J. Chem. Soc., Chem. Commun.* **1987**, 1066-1069. (d) Ballardini, R.; Balzani, V.; Clemente-Leon, M.; Credi, A.; Gandolfi, M. T.; Ishow, E.; Perkins, J.; Stoddart, J. F.; Tseng, H.-R.; Wenger, S. *J. Am. Chem. Soc.* **2002**, *124*, 12786-12795. (e) Huang, F.; Fronczek, F. R.; Gibson, H. W. *Chem. Commun.* **2003**, 1480-1481. (f) Reviews: Gibson, H. W. In *Large Ring Molecules*; Semlyen, J. A. Ed.; John Wiley & Sons: New York, 1996; Ch. 6, pp 191-262. Harada, A. *Acta Polym.* **1998**, *49,* 3-17. Raymo, F. M.; Stoddart, J. F. *Chem. Rev.* **1999**, *99*, 1643-1664. *Molecular Catenanes and Knots*; Sauvage, J.-P., Dietrich-Bucheker, C., Eds.; Wiley: New York, 1999. Mahan, E.; Gibson, H. W. In *Cyclic Polymers*, 2nd ed.; Semlyen, A. J. Ed.; Kluwer Publishers: Dordrecht, **2000**; pp 415-560. Hubin, T. J.; Busch, D. H. *Coord. Chem. Rev*. 2000, *200-202*, 5-52. Panova, I. G.; Topchieva, I. N. *Russ. Chem. Rev.* **2001**, *70*, 23-44.

4. (a) For examples of linear supramolecular polymers made in our lab see: Yamaguchi, N.; Nagvekar, D.; Gibson, H. W. *Angew. Chem. Int. Ed. Engl.* **1998,** *38*, 2361-2364; Gibson, H. W.; Yamaguchi, N.; J. W. Jones, *J. Am. Chem. Soc.* **2003**, *125,* 3522-3533. (b) For examples of dendritic self-assemblies see: Jones, J. W.; Bryant, W. S.; Bosman, A. W.; Janssen, R. A. J.; Meijer, E. W.; Gibson, H. W. *J. Org. Chem.* **2003**, *68*, 2385-2389; Gibson, H. W.; Yamaguchi, N.; Jones, J. W. *J. Am. Chem. Soc.* **2003**, *125,* 3522-3533.
5. (a) Bryant, W. S.; Jones, J. W.; Mason, P. E.; Guzei, I. A.; Rheingold, A. L.; Nagvekar, D. S.; Gibson, H. W. *Org. Lett.* **1999**, *1*, 1001-1004. The only other bicyclic hosts that have been used for pseudorotaxane/rotaxane syntheses are the glycouril-crown ether-porphyrin systems: (b) Rowan, A. E.; M. P. P.; K. W. Aarts,; Koutstaal, M. *Chem. Commun.* **1998**, 611-612. (c) Gunter, M. J.; Jeynes, T. P.; Johnston, M. R.; Turner, P.; Chen, Z. *J. Chem. Soc., Perkin 1* **1998**, 1945-1957. (d) Elemans, J. A. A. W.; Claase, M. B.; Aarts, P. P. M.; Rowan, A. E.; Schenning, A. P. H. J.; Nolte, R. J. M. *J. Org. Chem.* **1999**, *64,* 7009-7016.

6. Cram, D. J. *Science* **1988**, *240*, 760-767.
7. Bryant, W. S.; Guzei, I.; Rheingold, A. L.; Gibson, H. W. *Org. Lett.* **1999**, *1*, 47-50.
8. (a) Jones, J. W.; Zakharov, L. N.; Rheingold, A. L.; Gibson, H. W. *J. Am. Chem. Soc.* **2002**, *124*, 13378-13379. (b) Supramolecular cryptands have been referred to as "pseudocryptands". For the first such reference see: Nabeshima, T.; Inaba, T.; Sagae, T.; Furukawa, N. *Tetrahedron Lett.* **1990**, *31*, 3919-3922. For examples of recent references see: Romain, H.; Florence, D.; Alain, M. *Chemistry* **2002**, *8*, 2438-2445. Nabeshima, T.; Yoshihira, Y.; Saiki, T.; Akine, S.; Horn, E. *J. Am. Chem. Soc.* **2003**, *125*, 28-29. For a review see: Nabeshima, T.; Akine, S.; Saiki, T. *Rev. Heteroatom Chem.* **2000**, *22*, 219-239.
9. (a) Huang, F.; Zakharov, L. N.; Rheingold, A. L.; Jones, J. W.; Gibson, H. W. *Chem. Commun.* **2003**, 2122-2123. (b) Huang, F.; Guzei, I. A.; Jones, J. W.; Gibson, H. W. *Chem. Commun.* **2004**, Advance Article, Feb. 5th.
10. Gibson, H. W.; Nagvekar, D. S. *Can. J. Chem.* **1997**, *75,* 1375-1384.
11. Job, P. *Ann. Chim*. **1928**, *9*, 113-203.
12. Heath, R. E.; Dykes, G. M.; Fish, H.; Smith, D. K. *Chem. Eur. J.* **2003**, *9*, 850-855.
13. The highest value reported is 7.4 (±3.7) × 10^6 M^{-1} in 1:1 $CDCl_3$:CD_3CN (NMR titration).[5d]
14. Huang, F.; Gibson, H. W.; Bryant, W. S.; Nagvekar, D. S.; Fronczek, F. R. *J. Am. Chem. Soc.* **2003**, *125*, 9367-9371.
15. (a) Huang, F.; Fronczek, F. R.; Gibson, H. W. *J. Am. Chem. Soc.* **2003**, *125*, 9272-9273. (b) Huang, F.; Zhou, L.; Jones, J. W.; Gibson, H. W.; Ashraf-Khorassani, M. *Chem. Commun.* **2004**, 2670-2671.
16. Sheldrick, G.M. (**1998**), SADABS (2.01), Bruker/Siemens Area Detector Absorption Correction Program, Bruker AXS, Madison, Wisconsin, USA
17. Sheldrick, G. M. SHELXTL NT ver. 6.12; Bruker Analytical X-ray Systems, Inc.: Madison, WI, **2001**.
18. Altomare, A.; Cascarano, G.; Giacovazzo, C.; Guagliardi, A. *J. Appl. Cryst.* **1993**, *26*, 343-350.

19. Watkin, D. J.; Prout, C. K.; Carruthers, J. R.; Betteridge, P. W.; Cooper, R. I. CRYSTALS **2000**, Issue 11. Chemical Crystallography Laboratory, University of Oxford, Oxford.
20. Van der Sluis, P.; Spek, A. L. *Acta Cryst., Sect. A* **1990**, A46, 194-201
21. CrysAlis v1.170, Oxford Diffraction: Wroclaw, Poland, **2002**.

TOC Graphic:

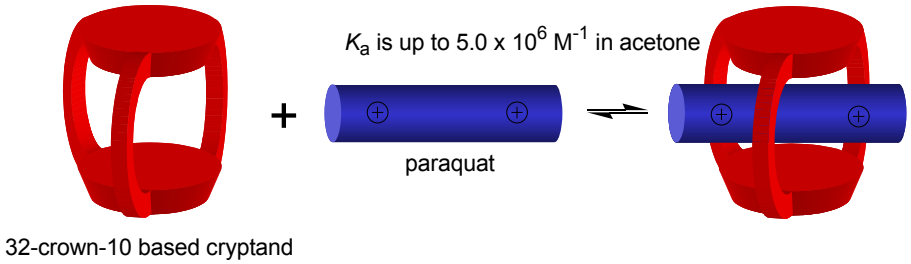

Abstract: Four new bis(*m*-phenylene)-32-crown-10 based cryptands with different third bridges were prepared. The complexes between them and paraquat derivatives were studied by proton NMR spectroscopy, mass spectrometry, and X-ray analysis. It was found that these cryptands bind paraquat derivatives very strongly. Specifically, a diester cryptand with a pyridyl nitrogen atom located at a site occupied by either water or a PF_6 anion in analogous complexes exhibited the highest association constant K_a = 5.0 $\times$ 10^6 M^{-1} in acetone with paraquat, 9000 times greater than the crown ether system. X-ray structures of this and analogous complexes demonstrate that improved complexation with this host is a consequence of preorganization, adequate ring size for occupation by the guest and the proper location of the pyridyl N-atom for binding to the β-pyridinium hydrogens of the paraquat guests. This readily accessible cryptand is one of the most powerful hosts reported for paraquats.